

## Role of Molecular Size in Ratchet Fractionation

Lotien Richard Huang,<sup>1</sup> Pascal Silberzan,<sup>4</sup> Jonas O. Tegenfeldt,<sup>3</sup> Edward C. Cox,<sup>3</sup> James C. Sturm,<sup>1</sup>  
Robert H. Austin,<sup>2</sup> and Harold Craighead<sup>5</sup>

<sup>1</sup>Center for Photonics and Optoelectronic Materials (POEM), Department of Electrical Engineering, Princeton University,  
Princeton, New Jersey 08544

<sup>2</sup>Center for Photonics and Optoelectronic Materials (POEM), Department of Physics, Princeton University,  
Princeton, New Jersey 08544

<sup>3</sup>Department of Molecular Biology, Princeton University, Princeton, New Jersey 08544

<sup>4</sup>Institut Curie, UMR CNRS 168-11, rue P & M Curie, 75005 Paris, France

<sup>5</sup>Department of Applied Physics, Cornell University, Ithaca, New York 14853

(Received 1 April 2002; published 4 October 2002)

We show the importance of finite particle size in microfluidic asymmetric continuous-flow diffusion arrays, specifically the critical nature of the particle size with respect to the barrier gaps. We show that particles much smaller than the barrier gap follow individual field lines through narrow gaps and are poorly fractionated. In contrast, particles comparable to the gap size lose memory of their incoming field line and can be fractionated with high resolution. We demonstrate this effect using a new technological approach to create very straight and narrow injection bands in such arrays, and completely resolve bands of DNA of lengths 48 500 and 167 000 base pairs.

DOI: 10.1103/PhysRevLett.89.178301

PACS numbers: 82.37.-j

The need for reliable and fast separation of large biomolecules such as DNA and proteins cannot be over-emphasized. Microfabricated structures have tried to exploit basic physical principles to demonstrate potential analytical tools for assaying biomolecules with high efficiency, but the details of particle flow in small patterned insulating structures is often ignored. It has been proposed that an array of spatially asymmetric obstacles could operate as a continuous-flow Brownian ratchet [1,2]. As particles drift through the obstacle array, they are selectively displaced perpendicular to their drift direction based on diffusion in the asymmetric structure. Experiments [3–5] showed that such asymmetric obstacle arrays can fractionate DNA molecules of high molecular weight ( $\sim 10^5$  base pair). However, because there are discrepancies between the theory [1,2] and the experimental results [4,5], it is not clear how the fractionation efficiency scales with molecular weight. While early theories proposed that smaller molecules should fractionate faster [1,2], a recent analysis [6] suggests that arrays of ion-impermeable obstacles could not serve as continuous-flow Brownian ratchets for pointlike particles. Thus, it remained questionable whether an ion-impermeable obstacle array could, in principle, fractionate small macromolecules (oligonucleotides, proteins, etc.), which are of great biological importance.

To probe this issue experimentally, DNA molecules of three sizes (411 bp, 48.5 kbp, and 167 kbp) were analyzed in an asymmetric obstacle array. Array boundary conditions of carefully aligned current were used to create very straight bands over long distances, and the separation of molecules was studied as a function of drift velocity. This Letter shows experimentally that fractionation in asymmetric obstacle arrays requires that the molecular

size be comparable with the barrier gap size, which is ignored in previous theories [1,2,6].

The conventional understanding of continuous-flow sorting by Brownian motion using asymmetric obstacle arrays [1,2] is shown in Fig. 1(a). Consider particles emerging from gap A driven towards gap B by an electric field. Executing biased random walks towards gap B, the particles spread out over the parabolic shaded region. While particles taking path 1 are blocked and deflected back to gap B, particles taking path 2 are deflected to gap B+. The probability of being deflected depends on the probability that a particle diffuses past the corner of an obstacle [point C in Fig. 1(a)], and thus is a function of the ratio between the width of the parabolic shaded region and the characteristic obstacle dimension [1]. This ratio may be written as a dimensionless parameter  $D/\nu a$ , where  $D$  is the particle's diffusion coefficient,  $\nu$  is its drift velocity, and  $a$  is the gap width between the obstacles. Since the deflection probability depends on

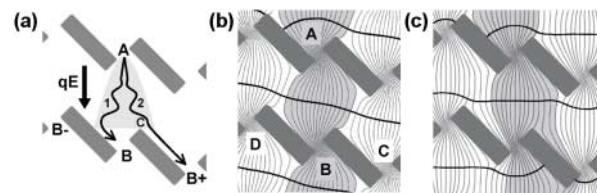


FIG. 1. (a) Basic principle of continuous sorting in an asymmetric array of obstacles. (b) Electric field and equipotential lines with boundary conditions that all field lines flow into gap A and continue through gap B. Note that the equipotential lines are not horizontal. (c) Field and equipotential lines with boundary condition of horizontal equipotentials. Note some field lines are diverted to adjacent gaps.

diffusion, particles of different diffusion coefficients should migrate in different directions. Based on theoretical calculation, Duke *et al.* suggested that, for the particular array geometry of Fig. 1(a),  $D/va$  of the molecules being separated should be between 0.02 and 0.3 for the best resolution, and the largest deflection probability should occur at  $D/va \sim 0.7$  [1].

Two major assumptions were made in the above model [1,2]: (i) There is no deflection of the electric field lines by the obstacles. (ii) The particles are assumed to have no physical size (pointlike particles). In the actual implementation of these arrays by microfabrication techniques [4,5], however, the obstacles consist of fused silica or other materials impervious to the ions in the fluid. Because the ions flow around the obstacle and the electric field  $\mathbf{E}$  is related to the ion flow  $\mathbf{J}$  by Ohm's law,  $\mathbf{J} = \sigma\mathbf{E}$ , where  $\sigma$  is the conductivity of the electrolytic fluid, the electric field lines go around the obstacles [Fig. 1(b)], violating the first of the above assumptions.

To isolate deflection due to diffusion, it is required that all field lines through an upper gap ["A" in Fig. 1(b)] map through a lower gap ("B"), which is aligned to the upper gap. If the field lines are misaligned so that some field lines through gap A leak to gap C or D [Fig. 1(c)], we will not be able to distinguish whether a particle migrating from gap A to C is by diffusion or by following the field. This requirement has to hold over the entire array area. This occurs only for a single choice of the angle of the equipotential lines. The proper equipotential contours [Fig. 1(b)] in our array were determined by numerically solving the Poisson equation using this field requirement as the boundary condition. Note that, although the average current flow is in the vertical direction [from A to B as shown in Fig. 1(b)], and the equipotential lines are always perpendicular to the local electric field by definition, they are not perpendicular to the average current direction and are not horizontal. If horizontal equipotentials are imposed as the boundary conditions [Fig. 1(c)], a significant proportion of molecules will drift to the right, even in the absence of diffusion.

To generate the desired aligned current distribution of Fig. 1(b), the array edges to which equipotentials are applied should be along the calculated equipotential direction. Therefore we designed our structure with properly slanted top and bottom edges (Fig. 2). The array was etched in fused silica by standard microfabrication methods and sealed with a glass cover slip to form the channels. For fabrication convenience, the structure was designed so that the direction of the calculated equipotential lines was parallel to the rows of obstacles, which we found by modeling not to be the case in general. Further, to ensure that the current pattern is highly aligned to the obstacles even in case of imperfect dimension control during microfabrication, the top and bottom array edges are not held at constant potentials with electrodes attached directly, but rather at constant current density with an array of current sources. In practice, the

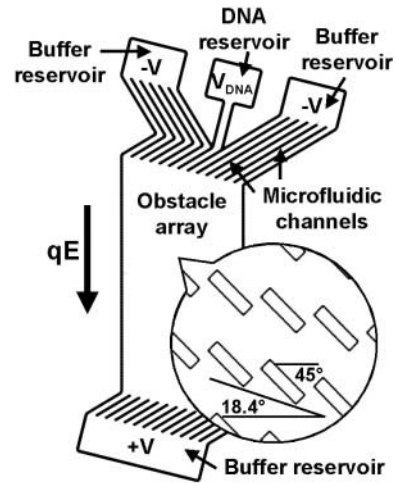


FIG. 2. Schematic diagram of the device.

current sources were implemented as an array of microfluidic channels with a high electrical resistance (compared to that of the array) connected to common fluid reservoirs (Fig. 2) [7]. Holes through the substrate allowed access to the reservoirs. The similar high voltage drop across all channels (compared to the small voltage drop in the array) leads to the same current flow in each channel at the boundary. A single extra channel connected to a special reservoir (with voltage calculated to give the same current as the other channels) was used to inject a  $90\text{-}\mu\text{m}$ -wide band of the molecules to be separated.

A mixture of coliphage  $\lambda$  DNA (48.5 kbp,  $\sim 5\ \mu\text{g}/\text{ml}$ ) and coliphage T2 DNA (167 kbp,  $\sim 2\ \mu\text{g}/\text{ml}$ ) in Tris-borate-EDTA buffer was injected into the array at various speeds using electric fields. The buffer contained 0.1% POP-6, a performance optimized linear polyacrylamide (Perkin-Elmer Biosystems) to suppress electroosmotic flow. At high fields ( $> 5\ \text{V}/\text{cm}$ ), diffusion was negligible ( $D/va < 0.05$  [8]), and as expected no lateral separation occurred [Fig. 3(a)]. The fact that the band did not curve even at the boundary of the array shows that the equipotential boundary conditions were properly imposed, and the current direction was well aligned to the obstacle array. Lateral separation of the two species was observed at a field strength lower than  $\sim 2\ \text{V}/\text{cm}$  ( $D/va > 0.13$  for coliphage  $\lambda$  DNA), with  $\lambda$  molecules being deflected from vertical more than those of T2. The separation became larger ( $\sim 1.3^\circ$ ) as the electric field was lowered to  $0.8\ \text{V}/\text{cm}$  [Fig. 3(b),  $D/va \sim 0.32$ ]. The drift velocity at fields less than  $0.8\ \text{V}/\text{cm}$  was so low ( $\sim 1\ \mu\text{m}/\text{s}$ ) that the stability of the separated bands became hard to maintain. The two species could be separated into two cleanly resolved bands 11 mm from the injection point, and the density profile of these bands was well fitted by two Gaussian peaks [Fig. 3(c)]. The resolution in the range of  $\sim 50\ \text{kbp}$  is  $\sim 30\ \text{kbp}$ , or  $\sim 60\%$  [9]. Although we did observe separation of molecules in the  $D/va$  range proposed by Duke *et al.* [1], the measured

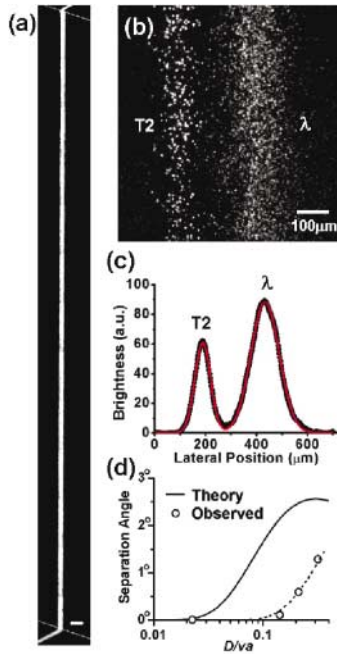


FIG. 3 (color). (a) Fluorescence micrograph of coliphage  $\lambda$  and T2 DNA stained with the fluorescent dye TOTO-1 forming a band of  $\sim 90 \mu\text{m}$  wide and 12 mm long at 12 V/cm. The slanted lines on the top and bottom mark the boundary of the obstacle array. Scale bar =  $300 \mu\text{m}$ . (b) Fluorescence micrograph of the two species separated into two bands 11 mm from the injection point using 0.8 V/cm. (c) Fluorescence profile of (b). Experimental data (thick black line) fitted with two Gaussian peaks (red). (d) Separation angle between  $\lambda$  and T2 bands as a function of the dimensionless parameter  $D/va$  of  $\lambda$  molecules. The solid curve is the theoretical prediction from Ref. [1]. Circles mark experiment data using electric fields of 12, 1.8, 1.2, and 0.8 V/cm. The dashed line is the theoretical curve empirically shifted to the right by a factor of 4.

separation was much smaller than the theoretical predictions [Fig. 3(d)].

To examine the scaling of the deflection to very small molecular sizes, a mixture of 411 bp (PCR product,  $\sim 1 \mu\text{g/ml}$ ) and  $\lambda$  DNA ( $\sim 20 \text{ ng/ml}$ ) was injected into the array, using electric fields ranging from 6 to 120 V/cm. At these field conditions,  $\lambda$  DNA molecules do not deviate from the field direction [Figs. 3(a) and 3(d)], and thus are used to label the field direction. The measured  $D/va$  for 411 bp molecules using 6 V/cm is  $\sim 0.8$  [10], so the corresponding  $D/va$  range tested is from 0.04 to 0.8, which covers the range where theory suggests best separation resolution ( $0.02 < D/va < 0.3$ ) [1] and maximum deflection ( $D/va \sim 0.7$ ). Therefore deflection should be observed for these smaller molecules. However, contrary to all expectations based on the theory [1,2], absolutely no lateral deflection was observed.

We believe that the reason the array failed to deflect small molecules (411 bp DNA) lies in the fact that small particles can precisely follow the electric field lines as they flow through the obstacle geometries [Fig. 4(a)].

Contrary to the basic principles of the diffusion array [1,2], where particles could widen out over the parabolic shaded region in Fig. 1(a) only via diffusion, small molecules will be spread out by the electric field. Particles now drift towards the vicinity of boundary  $L$  [via field line  $a$  in Fig. 4(a)] as well as to the boundary  $R$  (via field line  $c$ ). Thus, small molecules injected from a gap will have a much higher probability of diffusing to the left than the theory suggested [1,2]. In fact, a recent analysis showed that pointlike particles are equally likely to diffuse in both directions [6]. We summarize the argument as follows. For small particles that precisely follow electric field lines, their flux density  $\mathbf{J}_{\text{particle}}$  can be written as  $\mathbf{J}_{\text{particle}} = \rho\mu\mathbf{E} - D\nabla\rho$ , where  $\rho$  is the particle density,  $\mu$  is the mobility, and  $D$  is the diffusion coefficient. The first term of the flux density is due to the electric field, whereas the second term is from diffusion. According to the continuity equation, we have

$$-\frac{\partial\rho}{\partial t} = \nabla \cdot \mathbf{J}_{\text{particle}} = \mu\mathbf{E} \cdot \nabla\rho - D\nabla^2\rho. \quad (1)$$

Note we have used  $\nabla \cdot \mathbf{E} = 0$  because the electrolytic solution is neutral. If there is a high field so that the second term in Eq. (1) becomes relatively small, we find at steady state

$$\mathbf{E} \cdot \nabla\rho = 0. \quad (2)$$

This says the particle density is approximately constant along any field line. Thus, if one has a uniform concentration of particles arriving across all field lines

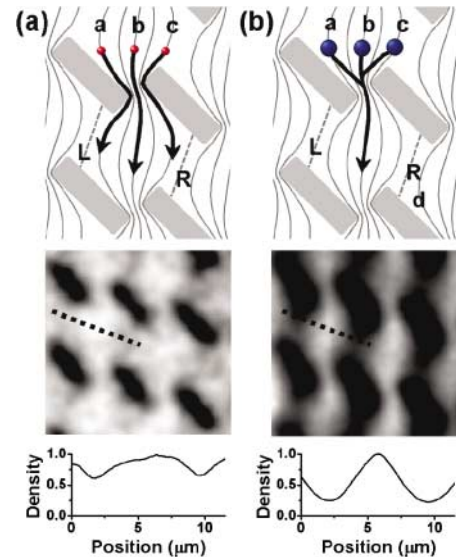


FIG. 4 (color). Schematic flow diagram and fluorescence image of particles in the center of the band for particles of size (a) 411 bp at average field of 120 V/cm and (b) 48.5 kbp (1.2 V/cm). The exposure time was long enough to show the particle density. The lower two images show brightness (normalized molecule density) vs position along the dotted lines of the fluorescent images.

entering a given gap (originating from a reservoir of uniform concentration), as the field lines (particle streamlines) widen out after the gap, the particle density will remain unchanged. This is illustrated in the fluorescence image of 411 bp DNA molecules in the array [Fig. 4(a)], which shows that DNA under high fields uniformly fills the entire space between rows of obstacles. Now, consider uniform injection of particles into all gaps at the top of the array using high fields, leading to uniform particle distribution in the array, and then we lower the field strength so that diffusion becomes important. Since all spatial derivatives of  $\rho$  in Eq. (1) are zero in our case of uniform density distribution, the particle density stays uniform according to Eq. (1), and thus the diffusion flux of particles across any field line must be equal to the inverse flux. Combined with translational symmetry, this implies that the probability of a particle diffusing across boundary  $L$  in Fig. 4(a) equals that across boundary  $R$ , a result which must hold for any distribution, not just for the assumed uniform distribution of particles. Given that there is no preferred direction of diffusion, there is no physical basis for ratcheting.

When a much larger  $\lambda$  DNA molecule approaches a gap, it is physically deflected by the obstacle and centered on the gap, because of its finite size (a random coil of  $\sim 1 \mu\text{m}$ ) compared to the gap width ( $\sim 1.4 \mu\text{m}$ ). Thus, molecules initially following field lines a, b, and c in Fig. 4(b) will all tend to leave the gap region on line b. The fluorescence image in Fig. 4(b) clearly shows this shadowing in contrast to Fig. 4(a) for the case of small molecules. Unlike 411 bp molecules, which are spread out in the space between rows of obstacles by the field,  $\lambda$  DNA molecules can only reach boundaries  $L$  and  $R$  in Fig. 4(b) by diffusion. Because boundary  $R$  is farther than boundary  $L$  from the gap where molecules emerge, molecules are more likely to diffuse across boundary  $R$ . Once a molecule reaches field line d, it will drift to the right. Therefore the obstacle array acts as a Brownian ratchet. The observed deflection is less than predicted by Ref. [1] [Fig. 3(d)]. Scaling the  $D/va$  value used by the theory by a factor of 4 brings the theory in close agreement with the data. This discrepancy occurs because the electric field funnels back most molecules that the theory counts as being deflected, such as particle C in Fig. 4(b).

In summary, this Letter clearly shows that, in a continuous-flow Brownian ratchet array, there exists a critical particle size threshold, which is related to the size of the narrowest feature through which the particles must pass in the array. Particles below this threshold maintain their flow along electric field lines through the gaps and are thus incapable of being ratcheted. Particles above this threshold size will be deflected from their original field lines by the obstacles, and can thus be ratcheted. Once

above this size, larger particles are ratcheted less because of their lower diffusion coefficient. This points to the importance of very narrow gaps in the obstacle array if the separation of small particles is desired.

This work was supported by grants from DARPA (MDA972-00-1-0031), NIH (HG01506), and the State of New Jersey (NJCS 99-100-082-2042-007). P. Silberzan gratefully thanks the DGA for financial support.

- 
- [1] T. A. Duke and R. H. Austin, Phys. Rev. Lett. **80**, 1552 (1998).
  - [2] D. Ertas, Phys. Rev. Lett. **80**, 1548 (1998).
  - [3] A. Oudenaarden and S. G. Boxer, Science **285**, 1046 (1999).
  - [4] C. F. Chou, O. Bakajin, S. Turner, T. Duke, S. S. Chan, E. C. Cox, H. G. Craighead, and R. H. Austin, Proc. Natl. Acad. Sci. U.S.A. **96**, 13762 (1999).
  - [5] M. Cabodi *et al.*, Electrophoresis (to be published).
  - [6] R. H. Austin, N. Darnton, R. Huang, J. Sturm, O. Bakajin, and T. Duke, Appl. Phys. A **75**, 279 (2002).
  - [7] L. R. Huang *et al.*, IEDM Technical Digest 363 (2001).
  - [8] In calculating the diffusion constants, we assume that coliphage  $\lambda$  DNA and T2 DNA molecules adopt random coil conformations. According to the approach used in Ref. [1] for calculating the diffusion coefficients,  $D_\lambda = 0.64 \mu\text{m}^2/\text{s}$ , and  $D_{T2} = 0.35 \mu\text{m}^2/\text{s}$ . The  $D/va$  values of experimental data are calculated using the measured velocities and  $a = 1.4 \mu\text{m}$ . The average velocities of T2 and  $\lambda$  DNA molecules were measured by tracing 20 individual molecules over many rows of obstacles using high magnification objectives. The mobilities derived from the velocities are  $\sim 1.8 (\mu\text{m/s})/(\text{V/cm})$  for  $\lambda$  DNA molecules, and  $\sim 1.9 (\mu\text{m/s})/(\text{V/cm})$  for T2 DNA molecules, which are comparable to the values reported in literature [4].
  - [9] J. C. Giddings, *Unified Separation Science* (Wiley, New York, 1991), pp. 101–106.
  - [10] Because 411 bp DNA molecules are not random coils, the parameter  $D/va$  was obtained by experimentally measuring the band broadening instead of using the method in Ref. [1]. Assuming that band broadening is not influenced by the obstacles, we used the following equations:  $t = y/v$  and  $\Delta x^2 = 2Dt + \Delta x_0^2$ , where  $y$  is the length of the band,  $\Delta x_0$  is the initial half-width of the band, and  $\Delta x$  is the half-width of the band after time  $t$ . Therefore,  $D/va = (\Delta x^2 - \Delta x_0^2)/2ya$ . At 6 V/cm,  $\Delta x_0 = 45 \mu\text{m}$  (measured at 1 mm) and  $\Delta x = 92 \mu\text{m}$  (at 4 mm), and thus  $D/va = 0.77$ . The diffusion coefficient extracted from this  $D/va$  value is  $\sim 12 \mu\text{m}^2/\text{s}$ , comparable to that reported in the literature [11]. The  $D/va$  values for higher fields were derived assuming constant mobility.
  - [11] N. C. Stellwagen, S. Magnusdottir, C. Gelfi, and P. G. Righetti, Biopolymers **58**, 390 (2001).